

Nano-montmorillonite Regulated Crystallization of Hierarchical Strontium Carbonate in a Microbial Mineralization System

Kui Zheng^{1,#}, Tao Chen^{2,3,#}, Jian Zhang^{2,3,#}, Xiuquan Tian², Huilin Ge², Tiantao Qiao², Jia Lei^{2,3}, Xianyan Li², Tao Duan^{2,3} and Wenkun Zhu^{2,3,*}

¹ Analytical and Testing Center, Southwest University of Science and Technology, Mianyang 621010, China; zhengkui@swust.edu.cn

² State Key Laboratory of Environmentally Friendly Energy Materials, Southwest University of Science and Technology, Mianyang 621010, China; chentao314710@163.com (T.C.); z2358727542@163.com (J.Z.); tian1993tian1993@163.com (X.T.); gehuilin1998@163.com (H.G.); 1805338097@qq.com (T.Q.); cutiancheng@163.com (J.L.); lxying@swust.edu.cn (X.L.); duant@ustc.edu.cn (T.D.)

³ Nuclear Waste and Environmental Safety Key Laboratory of Defense, National Collaborative Innovation Center for Nuclear Waste and Environmental Safety, Southwest University of Science and Technology, Mianyang 621010, China

* Correspondence: zhuwenkun@swust.edu.cn; Tel.: +86-816-608-9883

These authors contributed equally.

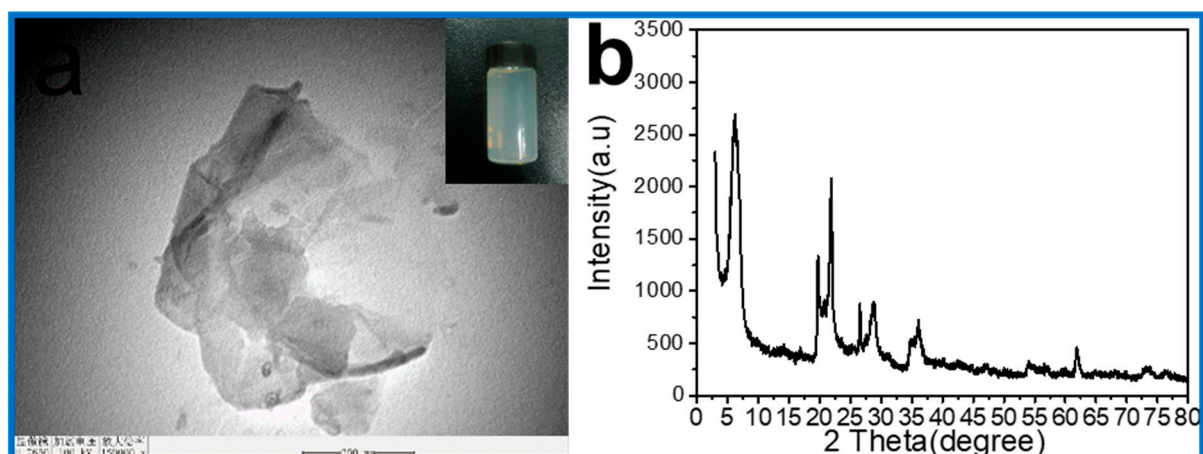


Figure S1. (a) TEM images of nano-MMT, where the inset shows pictures of nano-MMT suspension, (b) XRD patterns of nano-MMT.

The colony of *Bacillus pasteurii* on LB agar medium is characterized by smooth colonies, homogeneous edges, clear, elevated, viscous, see Figure S2a. *Bacillus pasteurii* is a spherical bacterium with a smooth surface and a size of 0.8–1.5 μm , see Figure S2b. The morphology of *Bacillus pasteurii* is distinctly different from that of calcite rods.

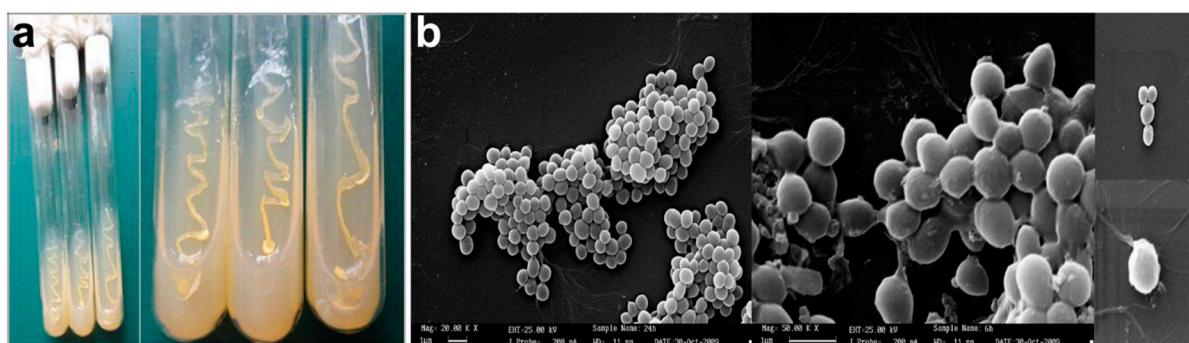


Figure S2. (a) *Bacillus pasteurii* colony, (b) SEM of *bacillus pasteurii* mycelium.

In the process of microbial mineralization of calcium carbonate, microorganisms play two core roles: One is to provide urease for urea hydrolysis, and the other is to provide crystal nuclei for the formation of calcium carbonate crystals [1,2,4,5]

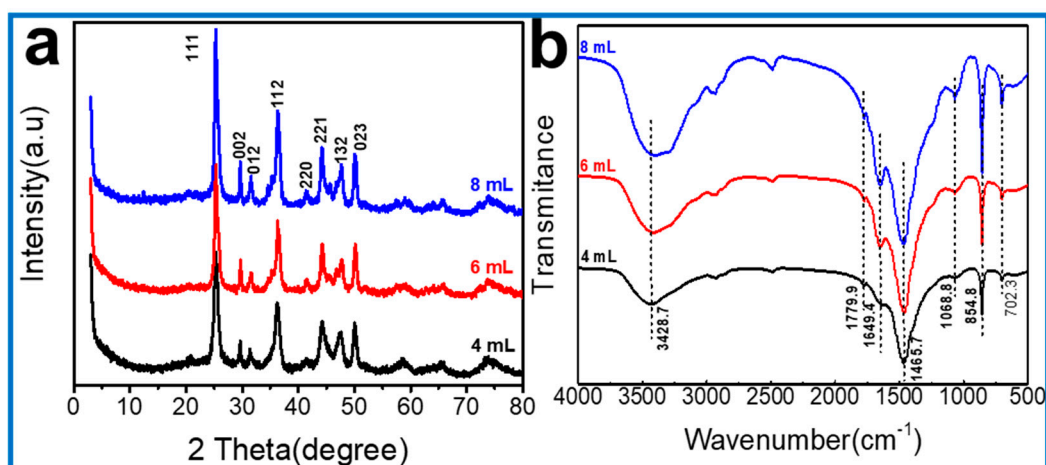
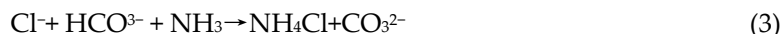
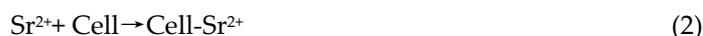


Figure S3. (a) XRD patterns and (b) FT-IR spectrum of strontium carbonate obtained using varying amounts of nano-MMT.

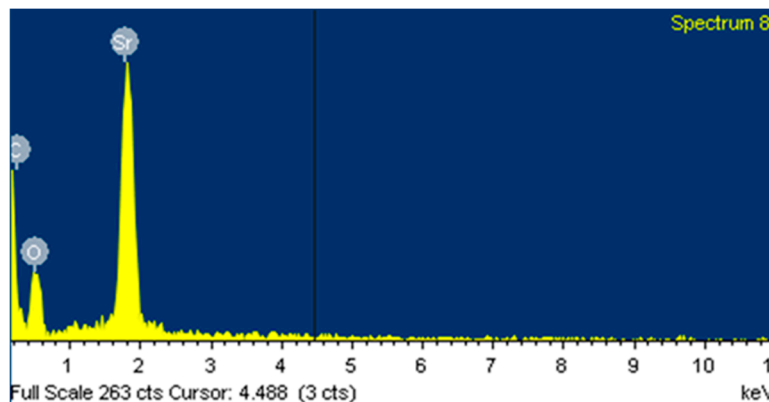


Figure S4. EDS spectrum of strontium carbonate.

Figure S5 shows the TGA data of strontium carbonate. The entire decomposition process was accompanied by three weight loss stages [3,6]. Weight lost slowly should be caused by the loss of water under 290 °C. Notable weight loss appeared in the curve during 313.5–776.3 °C, which should be caused by thermal decomposition of bacteria metabolite in the mineralized samples. The mineralized samples in the presence of nano-MMT have a weight loss rate of 5.0%, the mineralized samples in the absence of nano-MMT have a weight loss rate of 3.9%. Evidently, the weight loss rate of the mineralized samples in the presence of nano-MMT was 1.1% greater than the weight loss rate of the mineralized samples in the absence of nano-MMT, which should be attributed to the pyrolysis of nano-MMT in mineralized samples. Large thermal decomposition occurs at 776.3–985.6 °C, which can be attributed to the decomposition of strontium carbonate. From the analysis above, it is safe to conclude that the nano-MMT was involved in the crystallization process of strontium carbonate.

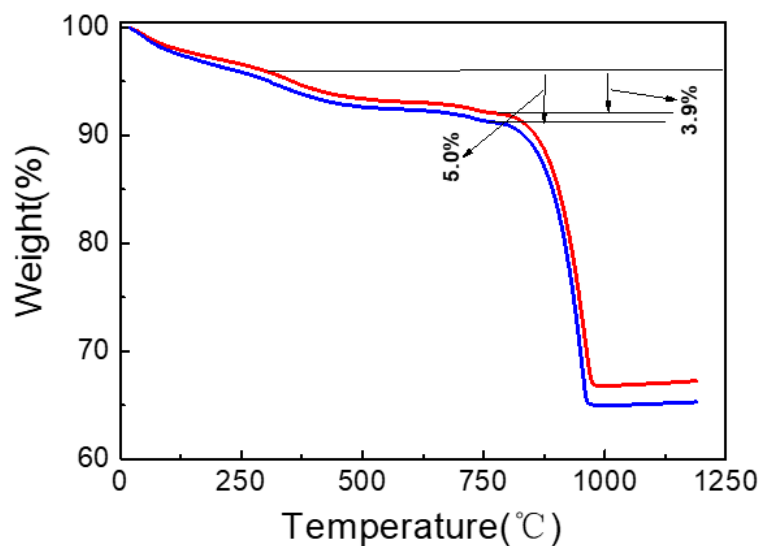


Figure S5. TGA spectra of mineralized samples in the absence of additives and the presence of nano-MMT, respectively.

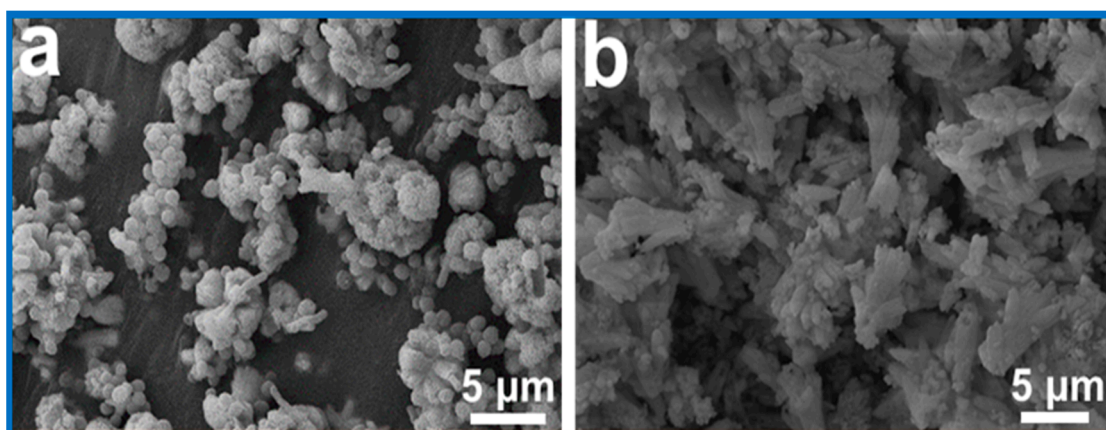


Figure S6. Typical SEM images of SrCO_3 were obtained by chemical method. (a) SrCO_3 were obtained in the water, (b) mineralized samples were obtained in the presence of Nano-MMT.

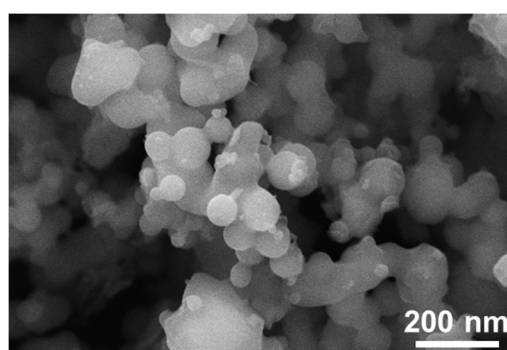


Figure S7. SEM of amorphous SrCO_3 precursor in the early stage of microbial mineralization.

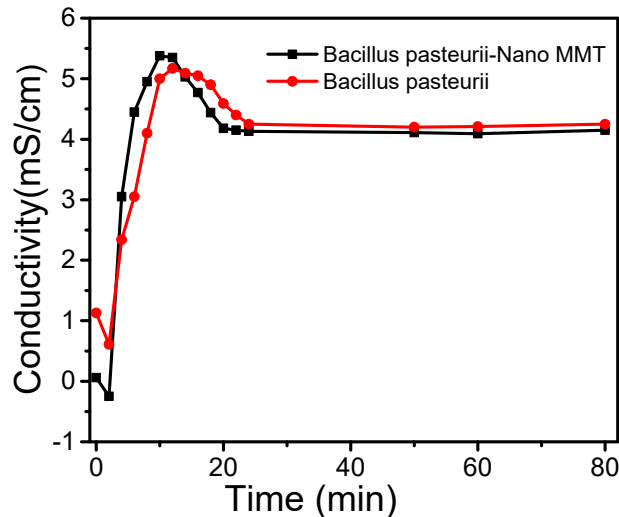


Figure S8. Relationship of conductivity with time in different mineralized solutions.

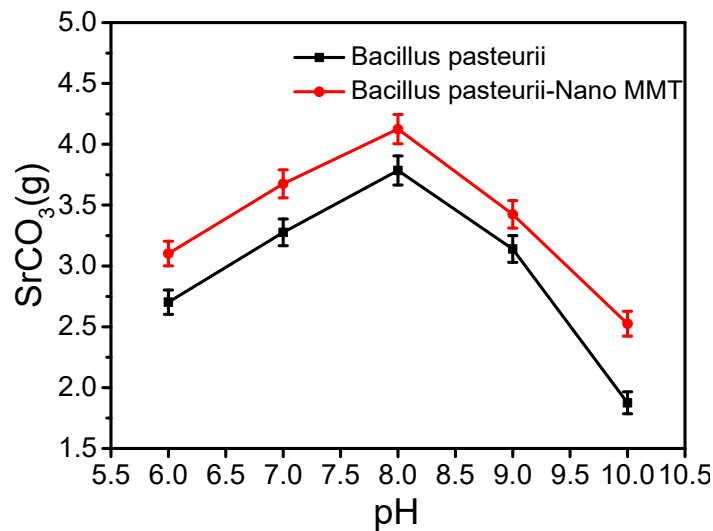


Figure S9. The effect of pH values on the yield of SrCO₃.

References

1. Dejong, J.T.; Fritzges, M.B.; Nüsslein, K. Microbially Induced Cementation to Control Sand Response to Undrained Shear. *J. Geotech. Geoenviron. Eng.* **2006**, *132*, 1381–1392.
2. Muynck, W.D.; Belie, N.D.; Verstraete, W.; Jonkers, H.M.; Loosdrecht, M.C.M.V. Microbial carbonate precipitation in construction materials: A review. *Ecolog. Eng.* **2010**, *36*, 118–136.
3. Chen, T.; Li, J.; Shi, P.; Li, Y.; Lei, J.; Zhou, J.; Hu, Z.; Duan, T.; Tang, Y.; Zhu, W. Effects of Montmorillonite on the Mineralization and Cementing Properties of Microbiologically Induced Calcium Carbonate. *Adv. Mater. Sci. Eng.* **2017**, *2017*, 1–13.
4. Chen, T.; Shi, P.; Li, Y.; Zhang, J.; Duan, T.; Yu, Y.; Zhou, J.; Zhu, W. Crystallization of calcium carbonate mineral with hierarchical structures regulated by silk fibroin in microbial mineralization system. *J. Cryst. Growth*, **2018**, *493*, 51–57.
5. Chen, T.; Shi, P.H.; Li, Y.; Duan, T.; Yu, Y.; Li, X.; Zhu, W. Biomining of Varied Calcium Carbonate Crystal by Synergistic Effect of Silk Fibroin/Magnesium ions in a Microbial System. *Crystengcomm* **2018**, *20*, 2366–2373.
6. Liu, L.; Zhang, X.; Liu, X.; Liu, J.; Lu, G.; Kaplan, D.L.; Zhu, H.; Lu, Q. Biomining of stable and monodisperse vaterite microspheres using silk nanoparticles. *ACS Appl. Mater. Interfaces* **2015**, *7*, 1735–1745.